ELSEVIER

Journal of Power Sources 105 (2002) 134–138

JOURNAL OF POWER SOURCES

www.elsevier.com/locate/jpowsour

Life duration of Ni–MH cells for high power applications

Laure Le Guenne*, Patrick Bernard

SAFT, 113 Boulevard Alfred Daney, 33074 Bordeaux Cedex, France

Abstract

Intensive research and development carried out at SAFT Research [1,2] has shown that limitation of Ni–MH battery life duration can be directly linked to AB_5 alloy corrosion in the negative electrode. A mathematical model taking into account these results has been developed in order to predict battery life as a function of the conditions of utilisation: cycle and calendar life [3].

However, the degradation of the negative electrode is the consequence of two phenomena: surface corrosion of the active alloy and decrepitation of alloy particles during cycling. Up to now, only the kinetic law controlling the evolution of the thickness of the corrosion layer could have been quantified [3]. On the other hand, the kinetic law of decrepitation could not be directly measured, but is only fitted by determining the total amount of corrosion.

Thus, an in situ method suitable to quantify the electrochemical surface of the alloy has been developed. Therefore, electrochemical impedance spectroscopy (EIS) has been used to follow the degradation of the negative electrode, as a function of depth of discharge (DOD) during cycling. Alloy corrosion measurements and scanning electron microscope (SEM) analyses have been performed to confirm the validity of the method. It has been found that decrepitation is nearly zero for low levels of low DOD (5%).

Keywords: Secondary battery; Nickel–metal hydride; Battery model; Impedance; Cycle life

1. Introduction

As it exhibits higher energy storage capabilities than nickel–cadmium at reasonable cost and does not show any safety issue, the nickel–metal hydride (Ni–MH) electrochemical system is predominant in a large range of portable appliances. For these reasons, the Ni–MH electrochemical system is also expected to be the energy source which will allow electric vehicles (EVs) to become an industrial reality.

One of the key points for the commercial success of Ni–MH batteries is life duration, especially for the EV application.

Fundamental results obtained at SAFT [1,2] have shown that the positive electrode endures no degradation during cycling and time and the limitation of Ni–MH battery life duration is directly linked to negative electrode degradation: corrosion and decrepitation of the alloy particles.

In the life duration model developed by SAFT [3], only the kinetic law controlling the evolution of the thickness of the corrosion layer has been taken into account. The kinetic law of decrepitation is not directly measured but only fitted by determining the total amount of corrosion. The expression used in the model is given in the following formula (law of corrosion in the mathematical model [3]):

$$\frac{\delta \text{corrosion}\,(t,\, T,\, \%)}{\delta t} = f\left(\frac{\delta e}{\delta t}, \frac{\delta S}{\delta t}, e, S, E_{\text{act}}\right) \quad (1)$$

where t is the time, T the cell temperature, % the discharged capacity, S the initial alloy surface area, E_{act} the activation energy and e the thickness of corrosion layer.

The methodology to establish this mathematical model is based on the quantification of the following parameters: the kinetic law controlling the evolution of the thickness of corrosion layer ($e(t)$), the activation energy determined from Arrhenius's law (E_{act}) and the kinetic law of decrepitation ($S(t)$).

Recently, SAFT has developed a new cylindrical Ni–MH 7 Ah D cell and 14 Ah 4/5 SF cell for high power applications, such as hybrid electrical vehicle (HEV) alterno-starter. The HEV alterno-starter application induces a very low depth of discharge (DOD) and a nearly constant state of charge (SOC). By the way, the present model developed for high DOD (80%) and variable SOC requires improvement in order to include the effect of SOC and DOD on alloy decrepitation and consequently on life duration.

Thus, an in situ method suitable to quantify alloy decrepitation needs to be developed. Electrochemical impedance spectroscopy (EIS) has been used to follow the degradation of the negative electrode.

* Corresponding author. Tel.: +33-557-106-819; fax: +33-557-106-877.
E-mail address: laure.le-guenne@saft.alcatel.fr (L.L. Guenne).

0378-7753/02/$ – see front matter
PII: S0378-7753(01)00931-4

Table 1
High power cylindrical Ni–MH range

	Tooling application			Automotive application	
	4/5 Cs	Cs	D	D auto	4/5 SF
Height (mm)	33	41.9	60.4	69.1	93
Diameter (mm)	23	23	32	32	41
Weight (g)	45	59	160	185	360
Capacity (Ah)	2	3	8.5	7	14
Energy (Wh)	2.4	3.6	10.2	8.5	17

To confirm decrepitation results observed by EIS measurements, alloy corrosion measurements and scanning electron microscope (SEM) analyses have been performed.

2. SAFT Ni–MH high power cylindrical performances

2.1. High power cylindrical Ni–MH range

SAFT has developed a large range of high power cylindrical Ni–MH range. By optimising the electrochemical and mechanical designs, power and energy densities have been increased. Specific electrochemical design has been developed: ultra-thin electrodes, optimised porosity of the electrochemical coil, high ionic conductivity electrolyte and optimised electrode composition to maximise conductivity and energy efficiency. A new mechanical design has been elaborated: internal nickel tabs are designed to pass up to 30 C discharge rate and external tabs are designed for high power and battery assembly.

The main characteristics (dimensions and performances) of SAFT's high power products range are summarised in Table 1.

2.2. Performances of high power cylindrical Ni–MH cells

The pictures of the D and 4/5 SF cells produced for automotive applications are presented in Figs. 1 and 2.

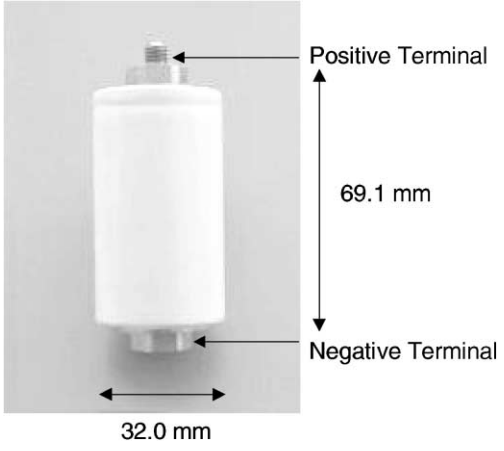

Fig. 1. D cell design.

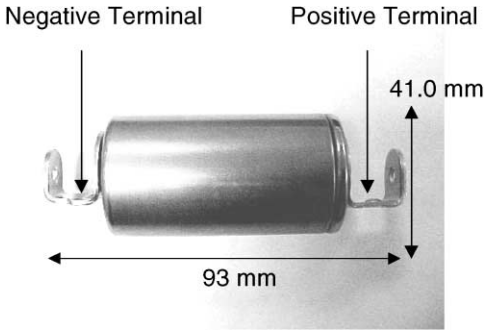

Fig. 2. 4/5 SF cell design.

Table 2
Performances of high power cylindrical Ni–MH cells (D and 4/5 SF)

Performances	D	4/5 SF
Typical power in discharge (W)		
5 s/23 °C	120	240
5 s/0 °C	60	120
Typical power in continuous charge (W) (23 °C)	60	120
Energy (rated)	8.5 Wh (7.0 Ah)	17 Wh (14.0 Ah)

Their main characteristics are summarised in Table 2. The energy is measured at C-rate at room temperature. The typical power in discharge is measured at room temperature at C-rate during 5 s, for $V > 0.7$ V. The typical power in continuous charge is measured at room temperature between 100 and 20% DOD.

A test is still running on D cell's cycle life and 200,000 cycles have been achieved without power regression (conditions of cycle life test: 5% DOD, charge at 3 C-rate, discharge at 18 C-rate during 2 s and 12 C-rate during 20 s, average SOC 80%).

3. Experimental

3.1. Experimental method

Ni–MH sealed cylindrical cells with a typical capacity of 1.2 Ah (AA size) were used for impedance measurements. These batteries were obtained by winding a nickel hydroxide positive electrode and a AB_5 hydrogen-storage alloy based negative electrode along with a polyolefin separator. The alloy composition is $MmNi_{3.55}Co_{0.75}Al_{0.3}Mn_{0.4}$ with $Mm = La_{0.33}Ce_{0.47}Nd_{0.15}Pr_{0.05}$.

Before EIS measurements were carried out, the cells were subjected to a defined number of cycles. The influence of DOD and rate of discharge on decrepitation were studied by varying cycling conditions ($5\% < \text{DOD} < 80\%$) which are summarised in Table 3. The average state of charge during cycling was 60%. The n C represent the theoretical rate suitable to discharge the cell in $1/n$ h.

Table 3
Cycling conditions

Series	DOD (%)	Rate of discharge (C)
A	5	1
B	20	1
C	50	1
D	80	1
E	80	3

After cycling test, impedance was measured at the same state of charge (SOC = 80%) after 1 h rest at the end of charge. Measurements were carried out in a 1000–0.1 Hz frequency range under galvanostatic mode, with a 50 mA amplitude alternating current (Autolab Ecochemie). The discharge current used during impedance measurement was set to *C*/5-rate. Each measurement was performed on three cells to confirm the reproducibility of the method.

The cycled electrodes were observed with a SEM (JSM 6330F field emission SEM) in order to correlate impedance measurements to alloy decrepitation. To quantify more accurately the decrepitation, a storage period of 8 weeks at 60 °C has been performed on AA cycled cells in order to enhance the alloy corrosion. The corrosion has been quantified by measuring the amount of corroded aluminium eluted by the hydride electrode and trapped in the positive electrode [2].

3.2. Impedance data analysis

Impedance data were analysed using a fitting program (Zview) which allowed each spectrum to be decomposed into elementary electrical components. Spectra are basically composed of two capacitive half circles which differ from conventional resistance–capacitance loops by the fact that their centres are not located on the real axis of the Nyquist complex plane plot. The electrical circuit used for the impedance fitting is illustrated on Fig. 3.

Equivalent impedance used for the impedance fitting is calculated using the following formula:

$$Z(\omega) = R_\infty + \frac{R_{LF}}{1 + R_{LF}C_{LF}(j\omega)^{\alpha_{LF}}} + \frac{R_{HF}}{1 + R_{HF}C_{HF}(j\omega)^{\alpha_{HF}}} \quad (2)$$

where R_{LF} and C_{LF} are the resistance and capacitance at low frequencies and R_{HF} and C_{HF} at high frequencies. R_∞ is the electrolyte and connections resistance.

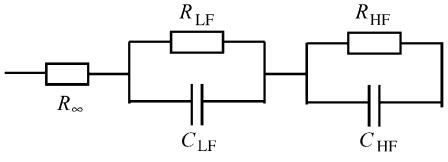

Fig. 3. Electrical circuit used for the impedance fitting.

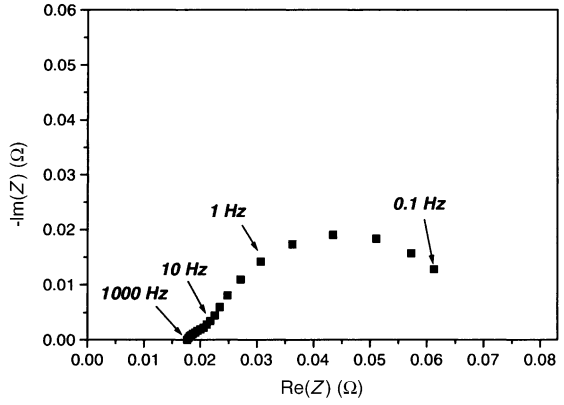

Fig. 4. Impedance diagram of a AA cell (state of charge close to 80%).

4. Results

4.1. EIS results

Impedance diagrams obtained on AA cells, in a 1000–0.1 Hz frequency range, are mainly composed of two capacitive loops (see Fig. 4).

Diagrams obtained for each series (see Table 3) at defined amount of discharged Ah were fitted using procedure described in previous paragraph.

Evolution of fitted electrical components (R_{LF}, C_{LF}, R_{HF}, C_{HF}) for each series as a function of number of discharged Ah is illustrated in Figs. 5–8.

Decrease of resistance as a function of discharged Ah is observed at high and low frequencies. Nearly linear increase is noticed for capacitance for both frequency ranges. R_∞ does not vary during cycling (300 Ah discharged) before separator drying.At high frequencies, we attribute R_{HF} and C_{HF} associated with the first loop, respectively to the charge transfer resistance and the double layer capacitance [4].

The interpretation of low frequency components depends on authors [5,6] but is always linked to electrochemical surface. The variation of alloy electrochemical surface can be quantified by determining $1/(R_{LF}/R_{LF\ initial})$.

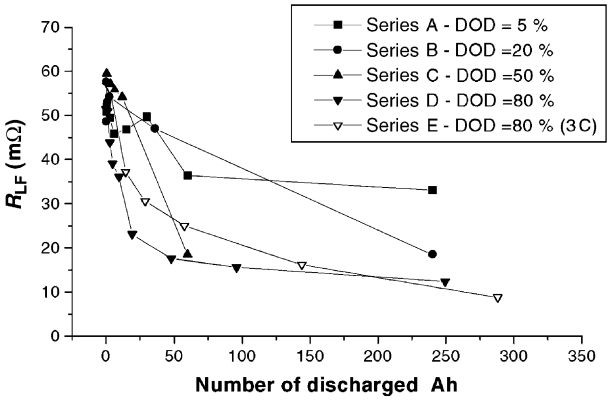

Fig. 5. Evolution of R_{LF} as a function of DOD and rate of discharge.

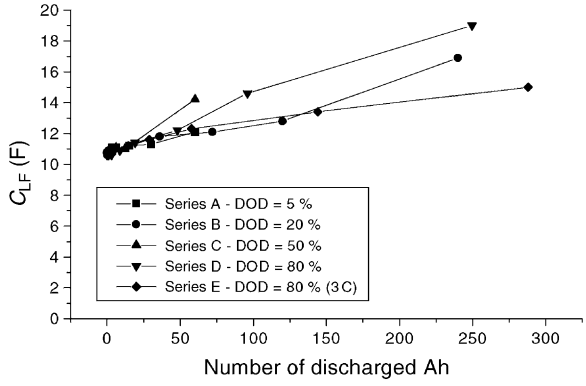

Fig. 6. Evolution of C_{LF} as a function of DOD and rate of discharge.

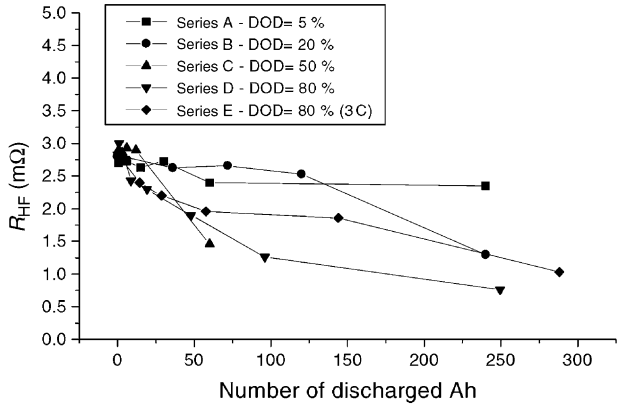

Fig. 7. Evolution of R_{HF} as a function of DOD and rate of discharge.

The Fig. 9 shows the evolution of $1/(R_{LF}/R_{LF\ initial})$ versus the number of discharged Ah. The electrochemical surface increases when DOD increases and is independent of rate of discharge during cycling. For high DOD values, the electrochemical surface is multiplied by a factor of four for this 10% Co alloy. For lower DOD values, the electrochemical surface remains nearly constant during cycling. It can be assumed that for low DOD, the level of stress inside the alloy particles is under the elasticity limit of the material and nearly no decrepitation occurs.

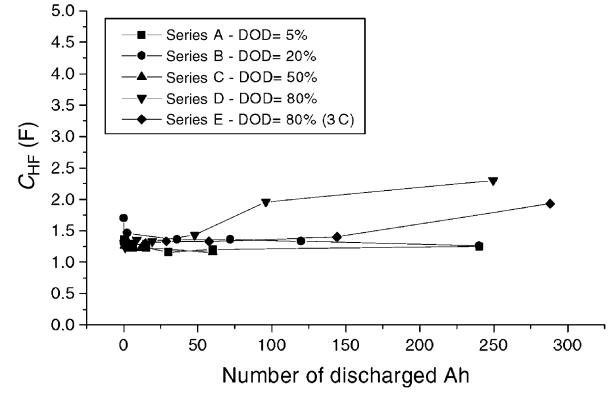

Fig. 8. Evolution of C_{HF} as a function of DOD and rate of discharge.

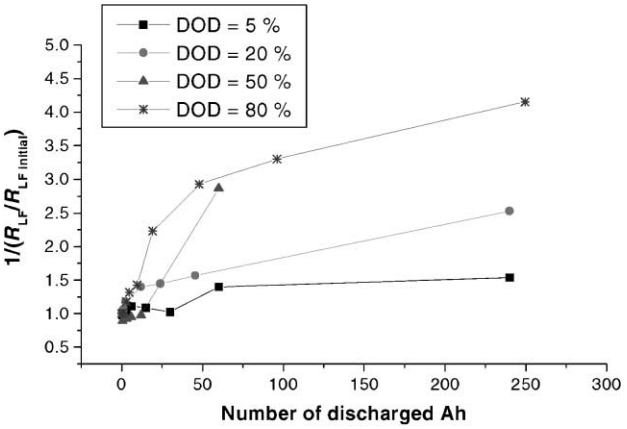

Fig. 9. Evolution of $1/(R_{LF}/R_{LF\ initial})$ as a function of number of discharged Ah.

In order to correlate these impedance measurements to alloy decrepitation, the cycled electrodes were then observed with a SEM and corrosion was measured on cycled AA cells.

4.2. SEM analyses

The cycled electrodes of the D-series (DOD = 80% at C-rate) were observed with a SEM for three defined number of cycles.

Fig. 10 illustrates the alloy particles before cycling ($R_{LF} = 55$ mΩ). Figs. 11 and 12 show respectively the decrepited alloy particles after 10 cycles (9.6 Ah discharged, $R_{LF} = 36.1$ mΩ) and after 100 cycles (96 Ah discharged, $R_{LF} = 15.6$ mΩ). An evaluation of the decrepitation has been performed using SEM analyses and p/S measurements (where p is the perimeter of particles and S the surface of particles measured by image analysis) [1]. The increase of p/S ratio between 0 and 100 cycles has been found equal to two which is close to the value obtained by EIS measurements.

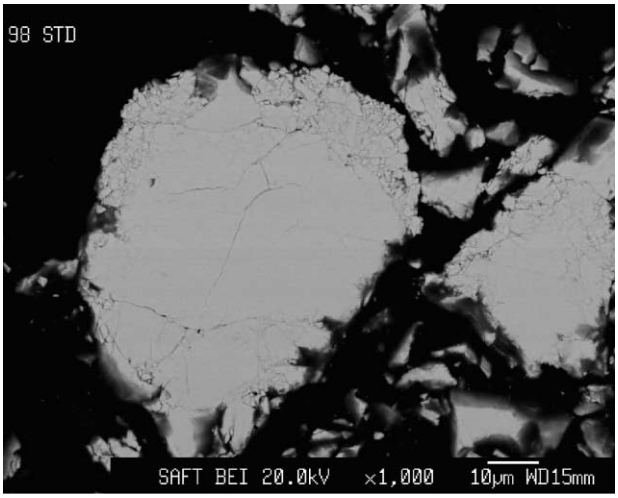

Fig. 10. SEM analyses on initial MH electrode.

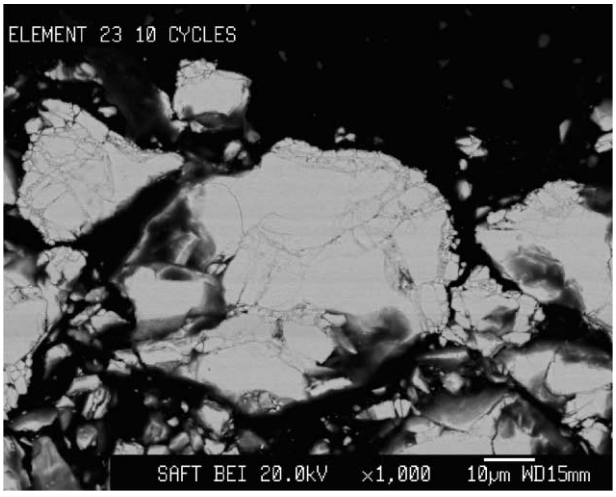

Fig. 11. SEM analyses on MH electrode after 10 cycles (9.6 Ah discharged).

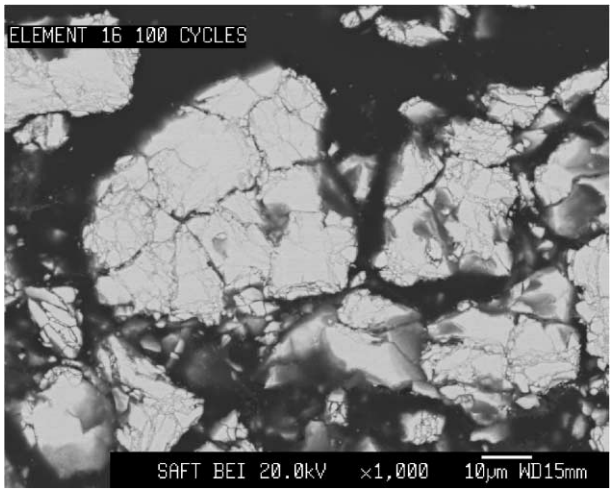

Fig. 12. SEM analyses on MH electrode after 100 cycles (96 Ah discharged).

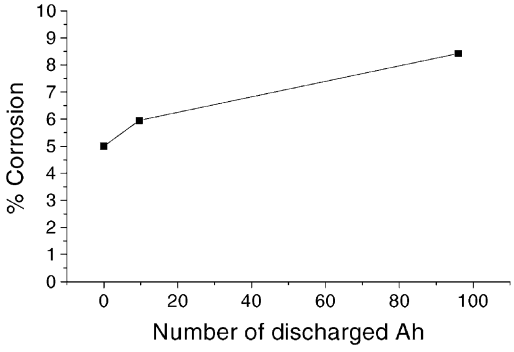

Fig. 13. Corrosion results as a function of discharged Ah after 8 weeks storage at 60 °C.

4.3. Corrosion measurements

To quantify more accurately the decrepitation kinetics during cycling, a storage period of 8 weeks at 60 °C has been performed on AA cycled cells in order to increase the alloy corrosion. Indeed, the corrosion level is proportional to active surfaces formed during cycling and will be enhanced during the storage period.

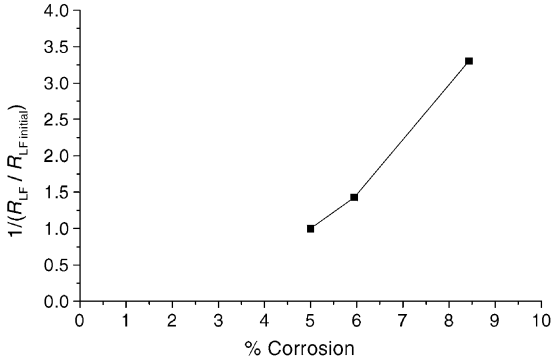

Fig. 14. R_{LF} measurements as a function of corrosion results after 8 weeks storage at 60 °C.

Corrosion measurements (see Figs. 13 and 14) confirm a good correlation between $1/(R_{LF}/R_{LF\ initial})$ and alloy corrosion after cycling and storage at 60 °C and consequently between $1/(R_{LF}/R_{LF\ initial})$ and alloy decrepitation. Thus, we can conclude that $1/(R_{LF}/R_{LF\ initial})$ determination is a method to quantify the alloy decrepitation.

5. Conclusions

It has been shown that EIS measurements and especially $1/(R_{LF}/R_{LF\ initial})$ determination is an accurate method for alloy decrepitation evaluation. SEM measurements and corrosion analyses have allowed the confirmation of the linking between R_{LF} and active surfaces formed during cycling. In this study, we have observed that the increase of $1/(R_{LF}/R_{LF\ initial})$ is faster when DOD increases and is independent of rate of discharge during cycling.

This new tool will help to measure the consequences of cycling parameters, such as SOC and electrode composition on life duration. For low DOD, the decrepitation law will be precisely determined in order to be implemented in the cycle life model.

References

[1] P. Leblanc, C. Jordy, B. Knosp, P. Blanchard, J. Electrochem. Soc. 144 (1998) 860–863.
[2] P. Bernard, J. Electrochem. Soc. 144 (1998) 456.
[3] C. Jordy, J.L. Liska, M. Saft, in: Proceedings of the 39th Conference on Power Sources, 12–15 June 2000.
[4] Internal results to be published.
[5] C. Wang, J. Electrochem. Soc. 145 (1998) 1801.
[6] N. Kuriyama, T. Sakai, H. Miyamura, H. Tanaka, I. Uehara, F. Meli, L. Schlapbach, J. Alloys Comp. 238 (1996) 128.